

1           **Estimating Surface Carbon Fluxes Based on a Local Ensemble**  
2           **Transform Kalman Filter with a Short Assimilation Window and a**  
3           **Long Observation Window: an OSSE test in GEOS-Chem 10.1**

4  
5       <sup>1,2</sup>Yun Liu, <sup>1</sup>Eugenia Kalnay\*, <sup>1</sup>Ning Zeng\*, <sup>3</sup>Ghassem Asrar, <sup>4</sup>Zhaohui Chen, <sup>5</sup>Binghao  
6       Jia

7  
8           1 Dept. of Atmospheric and Oceanic Science, University of Maryland – College Park

9           2 Dept. of Oceanography, Texas A & M university, College Station, TX

10          3 Joint Global Change Research Institute/PNNL, College Park, MD

11          4 School of Environmental Science, University of East Anglia, Norwich, UK

12          5 State Key Laboratory of Numerical Modeling for Atmospheric Sciences and  
13          Geophysical Fluid Dynamics (LASG), Institute of Atmospheric Physics, Chinese

14          Academy of Sciences, Beijing, China

15

16

17       \*Corresponding authors: [ekalnay@umd.edu](mailto:ekalnay@umd.edu), [zeng@umd.edu](mailto:zeng@umd.edu)

18

19

20

21

22

23

24

25

26

27

28

29

30

31

32

33

34

35

36

37

38

39

40

41

42

43

44

1  
2  
3  
4  
5  
6  
7  
8  
9  
10  
11  
12  
13  
14  
15  
16  
17  
18  
19  
20  
21  
22  
23  
24  
25  
26  
27  
28  
29  
30  
31  
32

**Abstract**

We developed a Carbon data assimilation system to estimate the surface carbon fluxes using the Local Ensemble Transform Kalman Filter and atmospheric transfer model GEOS-Chem driven by the MERRA-1 reanalysis of the meteorological field based on the Goddard Earth Observing System Model, Version 5 (GEOS-5). This assimilation system is inspired by the method of Kang et al. [2011, 2012], who estimated the surface carbon fluxes in an Observing System Simulation Experiment (OSSE) mode, as evolving parameters in the assimilation of the atmospheric CO<sub>2</sub>, using a short assimilation window of 6 hours. They included the assimilation of the standard meteorological variables, so that the ensemble provided a measure of the uncertainty in the CO<sub>2</sub> transport. After introducing new techniques such as “variable localization”, and increased observation weights near the surface, they obtained accurate surface carbon fluxes at grid point resolution. We developed a new version of the LETKF related to the “Running-in-Place” (RIP) method used to accelerate the spin-up of EnKF data assimilation [Kalnay and Yang, 2010; Wang et al., 2013, Yang et al., 2014]. Like RIP, the new assimilation system uses the “no-cost smoothing” algorithm for the LETKF [Kalnay et al., 2007b], which allows shifting at no cost the Kalman Filter solution forward or backward within an assimilation window. In the new scheme a long “observation window” (e.g., 7-days or longer) is used to create an LETKF ensemble at 7-days. Then, the RIP smoother is used to obtain an accurate final analysis at 1-day. This new approach has the advantage of being based on a short assimilation window, which makes it more accurate, and of having been exposed to the future 7-days observations, which accelerates the spin up. The assimilation and observation windows are then shifted forward by one day, and the process is repeated. This reduces significantly the analysis error, suggesting that the newly developed assimilation method can be used with other Earth system models, especially in order to make greater use of observations in conjunction with models.

Key words: Carbon Data Assimilation, Surface Carbon Flux, LETKF

1  
2  
3  
4  
5  
6  
7  
8  
9  
10  
11  
12  
13  
14  
15  
16  
17  
18  
19  
20  
21  
22  
23  
24  
25  
26  
27  
28  
29  
30  
31

## 1. Introduction

The exchange of carbon among atmosphere, land and oceans contributes to changes in the Earth’s climate, and is also sensitive to climate conditions. The CO<sub>2</sub> concentration in the atmosphere is affected by both the natural variability of the Earth’s planetary system, and anthropogenic emissions. The terrestrial and oceanic ecosystems absorb more than one-half of the anthropogenic CO<sub>2</sub> emission [Le Quéré *et al.*, 2016]. One major scientific question is whether this rate of removal of CO<sub>2</sub> from atmosphere will continue in future, and can it be enhanced? It is thus essential to better quantify the dynamics of earth surface carbon fluxes (SCF), and the variations of carbon sources and sinks, and their associated uncertainties.

A common approach for estimating SCF from atmospheric CO<sub>2</sub> measurements and atmospheric transport models is referred to as a “top-down” approach. The “top-down” methods estimate SCF through techniques such as Bayesian synthesis approach [Rödenbeck *et al.*, 2003; Gurney *et al.*, 2004; Enting, 2002; Bousquet *et al.*, 1999], different types of ensemble Kalman filters (EnKF) [e.g. Peters *et al.*, 2005, 2007; Feng *et al.*, 2009; Zupanski *et al.* 2007; Lokupitiya *et al.*, 2008], or variational data assimilation method [e.g., Baker *et al.*, 2006, 2010; Chevallier *et al.*, 2009].

Kang *et al.* [2011, 2012] developed a “top-down” carbon data assimilation system by coupling an atmospheric general circulation model (AGCM), including atmospheric CO<sub>2</sub> concentrations, with the Local Ensemble Transform Kalman Filter (LETKF) [Hunt *et al.*, 2007]. The meteorological variables (wind, temperature, humidity, surface pressure) and CO<sub>2</sub> concentrations were assimilated simultaneously in order to account for the uncertainties of the meteorological field, and their impact on the transport of atmospheric CO<sub>2</sub>. They carried out Observing System Simulation Experiments (OSSEs), and their carbon assimilation system achieved for the first time an accurate estimation of the evolving SCF at the model grid resolution, without requiring any *a priori* information. The surface carbon fluxes were considered as “unobserved evolving parameters”, by augmenting the state vector at each column with a surface carbon flux (SCF). The Local Ensemble Transform Kalman Filter (LETKF) then estimated this evolving parameter from the error covariance between the low level atmospheric CO<sub>2</sub> and the estimated SCF, and

1 after a spin-up of about one month, the LETKF accurately recovered the nature run  
2 seasonal surface carbon fluxes.

3 Kang et al., [2011, 2012] used a short 6-hour assimilation window for both  
4 atmospheric and CO<sub>2</sub> observations because atmospheric observations are usually  
5 assimilated at this frequency, and because most Ensemble Kalman Filter methods require  
6 short windows to ensure that the forecast perturbations growth remains linear. Such a short  
7 data assimilation window, required by the LETKF, also protects the system from becoming  
8 ill conditioned [Enting, 2002, Fig. 1.3], and as a result it does not require additional *a priori*  
9 information. We note further that the use of such a short assimilation window differs very  
10 much from most other “top-down” approaches for estimating SCF that use long  
11 assimilation windows varying from a few weeks to months [e.g., Baker et al., 2006, 2010;  
12 Peters et al., 2005, 2007; Michalak, 2008; Feng et al., 2009].

13 Although the Kang et al. methodology was successful, it is computationally  
14 expensive, requiring ensemble forecasts and data assimilation not only for the carbon  
15 variables, but also for the standard atmospheric variables, in order to estimate the  
16 uncertainties of the CO<sub>2</sub> atmospheric transport process. In this study, we used an improved  
17 version of LETKF data assimilation system with a state-of-the-art atmospheric transport  
18 model, the GEOS-Chem [Bey et al., 2001; Nassar et al., 2013], which is driven by the  
19 MERRA-1 reanalysis of the Goddard Earth Observing System Model, Version 5 (GEOS5).  
20 The improved data assimilation system, unlike Kang et al [2011, 2012], does not include  
21 an estimation of transport uncertainties related to the meteorological field.

22 The ultimate goal of our LETKF\_C system is to estimate the grid-point SCFs,  
23 which, as in Kang et al. [2011, 2012], are treated as time-evolving parameters in the system.  
24 As mentioned before, an Ensemble Kalman Filter requires a short assimilation window in  
25 order to have the ensemble perturbations evolve linearly and remain Gaussian. On the other  
26 hand, it is well known that the training needed to estimate evolving parameters through  
27 data assimilation could be quite long, so that it benefits from having many observations.  
28 Therefore, a short assimilation window would shorten the training period needed for the  
29 estimation of the SCF error covariance, hence lengthen the spin-up time.

30 To address this problem, we developed a new version of the LETKF using the  
31 “Running-in-Place” (RIP) method to accelerate the spin-up of EnKF data assimilation

1 [Kalnay and Yang, 2010; Wang et al., 2013; Yang et al., 2012]. Like RIP, the new  
2 assimilation system uses the “no-cost smoothing” algorithm [Kalnay et al., 2007b] that  
3 allows shifting at a negligible cost of the Kalman Filter solution forward or backward  
4 within a given assimilation window. Briefly, the new scheme works like this: a long  
5 “observation window” (e.g., 7-days, containing all the observations within 7 days) is used  
6 to create a temporary LETKF ensemble analysis at 7-days. Then the RIP smoother is used  
7 to obtain a final analysis at 1-day. This analysis has the advantage of being based on a short  
8 assimilation window, which makes it more accurate, and of having been exposed to the 7-  
9 days of observations, which accelerates the spin up time. The assimilation and observation  
10 windows are then shifted forward by one day, and the process is repeated. We have tested  
11 this new method (short assimilation, long observation window) achieving a significant  
12 reduction of analysis errors, and we believe that this method could be useful in other data  
13 assimilation problems.

14 This paper is organized as follows: Section 2 briefly describes the new system used  
15 for CO<sub>2</sub> data assimilation (LETKF\_C). Section 3 explores the effect of combining  
16 assimilation and observation windows in an OSSE framework. Section 4 presents results  
17 of the proposed methodology applied to CO<sub>2</sub> data. A summary and discussion are  
18 presented in section 5.

19

## 20 **2. LETKF\_C data assimilation system**

21 A data assimilation system includes a forecast model, observations, and a data  
22 assimilation method that optimally combines them. In the proposed LETKF\_C data  
23 assimilation system we use the GEOS-Chem as the forecast model and LETKF as the data  
24 assimilation method. The pseudo-observations for our OSSE experiments are created at  
25 the locations of the real carbon observations from Orbiting Carbon Observatory-2 (OCO-  
26 2) satellite [Crisp et al., 2004].

27

### 28 **2.1 GEOS-Chem model and the “nature” run**

29 GEOS-Chem is a global 3-D atmospheric Chemical transport model driven by the  
30 NASA reanalysis (MERRA-1) meteorological fields from the Goddard Earth Observing  
31 System data assimilation System Version 5, by the NASA Global Modeling and

1 Assimilation Office [Bosilovich et al., 2015]. This model has been applied worldwide to  
2 a wide range of atmospheric composition and transport studies. The GEOS-Chem model  
3 used in this study is the version v10-01 with a resolution of  $4^\circ \times 5^\circ$  (latitude x longitude),  
4 and 47 hybrid pressure-sigma vertical levels for CO<sub>2</sub> simulation [Nassar et al., 2013].  
5 GEOS-Chem is driven by the MERRA-1 reanalysis with 72 hybrid vertical levels,  
6 extending from the surface up to 0.01 hPa. The data used in this study was provided by the  
7 GEOS-Chem support team, based at the Harvard and Dalhousie Universities with support  
8 from the NASA Earth Science Division and the Canadian National and Engineering  
9 Research Council, who re-gridded the original data of spatial resolution of  $0.25^\circ \times 0.3125^\circ$   
10 into the resolution of  $4^\circ \times 5^\circ$ .

11 GEOS-Chem requires the SCFs as a set of parameters at each grid point in order to  
12 simulate the CO<sub>2</sub> concentration in the atmosphere. It is not possible to observe the global  
13 SCFs directly. Therefore, the SCFs are created from a “bottom-up” approach (considered  
14 as “truth” in our experiments) and used for the simulation of atmospheric CO<sub>2</sub>  
15 concentration with GEOS-Chem. The “bottom-up” SCFs used in this study include the  
16 three components shown in Equation (1): 1) terrestrial carbon fluxes ( $F_{TA}$ ); 2) air-sea  
17 carbon fluxes ( $F_{OA}$ ); 3) anthropogenic fossil fuel emissions ( $F_{fe}$ ).

$$18 \quad SCF = F_{TA} + F_{OA} + F_{fe} \quad (1)$$

19 The  $F_{TA}$  values are derived from the VEgetation Global Atmosphere Soils (VEGAS)  
20 model [Zeng et al., 2004; Zeng et al., 2005], forced by the real evolving weather, obtained  
21 from the GEOS-Chem. The  $F_{OA}$  values are from Takahashi et al. [2002], a climatological  
22 seasonal cycle estimated for the 1990s, and the  $F_{fe}$  values are from Fossil Fuel Data  
23 Assimilation System (FFDAS) for the year 2012 [Asefi-Najafabady et al., 2014]. The air-  
24 sea carbon flux and  $F_{fe}$  values were scaled using the global carbon budget data of Le Quéré  
25 et al. [2015], in order to include interannual variations. A nature run for atmospheric CO<sub>2</sub>  
26 concentration simulation is driven by the SCFs in units of  $(\frac{kgC}{m^2yr})$  based on all three datasets.

27 In OSSEs, the nature run serves as the “truth”. We assume that the true “bottom-up”  
28 carbon fluxes are not known in our data assimilation experiments, and they will be  
29 estimated using the atmospheric pseudo-observations derived from the “truth”, as  
30 described in more detail below. The nature run obtained by coupling GEOS-Chem with

1 VEGAS is fairly realistic [figure not shown], so we use it to create the pseudo OCO-2  
2 observations for the period of January 2015- March 2016.

### 3 **2.2 Pseudo-Observations**

4 The ultimate goal of this model-data assimilation system is to estimate the SCFs at  
5 every grid point using real observations such as the conventional surface CO<sub>2</sub>  
6 measurements of GlobalViewplus (GV+) flask network provided by Cooperative Global  
7 Atmospheric Data Integration Project [2016], and the observations from satellites such as  
8 the Greenhouse Gases Observing Satellite (GOSAT) [Yokota et al., 2004], and the Orbiting  
9 Carbon Observatory-2 (OCO-2) [Crisp et al., 2004]. Therefore, it is very beneficial to  
10 choose a realistic observation network to generate the pseudo-observation for testing the  
11 proposed data assimilation system. In this study, we developed the pseudo-observations  
12 for the OSSE assimilation experiments based on a realistic OCO-2 observation product.

13 The OCO-2 observations are the CO<sub>2</sub> column-averaged dry air mole fractions over  
14 the entire OCO-2 pixel (defined as X<sub>co2</sub>). The synthetic observations cover the entire globe  
15 once every 14 days with very high spatial resolution. It includes 24 samples per second  
16 along the satellite track within ~ 7 km span. The observations are expected to be highly  
17 correlated over a short length scale. Furthermore, the observation quality is greatly affected  
18 by conditions such as cloud cover, surface type and the solar zenith angle at the time of  
19 measurement. The OCO-2 retrieval algorithm uses a warning level (WL) between 0 and 19  
20 to indicate the quality of measurements, where WL=0 means “most likely good”, and  
21 WL=19 means “least likely good” observations. To avoid highly correlated measurements  
22 being treated as independent measurements and to bring the spatial resolution in line with  
23 the resolution of atmosphere transfer model, David Baker provided an OCO-2 observation  
24 dataset which averaged the synthetic X<sub>co2</sub> in 10-second time window using the “good  
25 quality” observations retrieval defined by WL ≤ 15 (personal communication).

26 The OCO-2 retrievals used to obtain averages are based on the NASA Atmospheric  
27 CO<sub>2</sub> Observations from Space XCO<sub>2</sub> retrieval Algorithm version7r (O'Dell et al., 2012),  
28 as archived at [https://disc.gsfc.nasa.gov/datasets/OCO2\\_L2\\_Lite\\_FP\\_7r/summary](https://disc.gsfc.nasa.gov/datasets/OCO2_L2_Lite_FP_7r/summary) (last  
29 access: 23 March 2017). A two-step averaging method has been used in order to avoid the  
30 final average to be disproportionately weighted to one part of the averaging bin (track) with  
31 more good quality retrievals. In the first step, the “good quality” retrievals defined as

1 WL $\leq$ 15 and xco2\_quality\_flag=0 (another quality indicator of the data) are averaged over  
2 1-second bins, with weights inversely proportional to the square of each retrievals posterior  
3 uncertainty. In the second step, all the 1-second bins, with at least one valid retrieval, are  
4 averaged over a 10-second interval to create 10-second averaged data. The OCO-2  
5 averaging kernels are similarly averaged to create 10-second mean averaging kernels. This  
6 averaging method had been used for similar purpose in the recent study by Basu et al.  
7 (2018). In this study, we further aggregated the observations from David Baker at the  
8 nearest GEOS-Chem output time of the 0, 6, 12, 18 UTC for each model day. The typical  
9 one-day coverage of observation of OCO-2 is shown in Figure 1. The values of Xco2 in  
10 the winter are significantly larger than those in summer of the Northern hemisphere and  
11 the OCO-2 observations are missing in the winter, for middle and high latitude regions  
12 (latitude  $>$   $\sim$ 30). We used the actual location, time and error scales of the OCO-2  
13 observations to create the pseudo-observations for our experiment. The pseudo-  
14 observations are created by obtaining the “true” CO<sub>2</sub> from the “nature” run using the  
15 location and time of the valid observation, then adding random errors with due  
16 consideration to the scales of the corresponding real observations. These derived pseudo-  
17 observations used in this study are based on the real observations associated error scales ,  
18 thus are more realistic than the GOSAT observations also used in Kang et al. [2012],  
19 because they are anchored, for example, to the real OCO-2 observations and to their quality,  
20 and their statistical representation.

21

### 22 **2.3 The LETKF data assimilation system**

23 The ensemble Kalman filter (EnKF) is a powerful tool for data assimilation that  
24 was first introduced by Evensen [1994]. The key attribute of this method is to derive the  
25 forecast uncertainties from an ensemble of integrated model simulations. A variety of  
26 ensemble Kalman filter assimilation methods have been proposed [Burgers et al., 1998;  
27 Houtekamer and Mitchell, 1998; Anderson, 2001, 2003; Bishop et al., 2001; Whitaker and  
28 Hamill, 2002; Tippett et al., 2003; Ott et al., 2004, Hunt et al., 2004]. The Local Ensemble  
29 Transform Kalman Filter (LETKF) introduced by Hunt et al. [2007] is chosen for this study.

30 The LETKF is an extension of the Local Ensemble Kalman Filter [Ott et al., 2004]  
31 with the implementation of the ensemble transform filter [Bishop et al., 2001; Wang and



1 Bishop, 2003]. It is widely used for data assimilation, including several operational centers,  
 2 and was also used for carbon data assimilations by Kang et al. [2011, 2012].

3 As discussed earlier, we follow Kang et al., [2011] in estimating the SCFs as  
 4 evolving parameters, augmenting the state vector  $C$  (the prognostic variable of atmospheric  
 5 CO<sub>2</sub>) with the parameter SCF, i.e.,  $X = [C, SCF]^T$ . The analysis mean  $\bar{X}^a$  and its ensemble  
 6 perturbations  $X^a$  are determined by Equations (2.1, 2.2) at every grid point, and the  
 7 ensemble analysis is used as initial conditions for the ensemble forecast in the next cycle.

$$8 \quad \bar{X}^a = \bar{X}^b + X^b \tilde{K} (y^o - \bar{y}^b) \quad (2.1)$$

$$9 \quad X^a = X^b [(K - 1) \tilde{P}^a]^{1/2} \quad (2.2)$$

10 Here  $\bar{X}^b$  is the mean of the forecast (background) ensemble members;  $X^b$  is a  
 11 matrix whose columns are the background perturbations of  $X_k^b - \bar{X}^b$  for each ensemble  
 12 member  $X_k^b$  ( $k=1, \dots, K$ ), where  $K$  is the ensemble size;  $y^o$  is a vector of all the observations;  
 13  $\bar{y}^b$  is the background ensemble mean in observation space ( $\bar{y}^b = H(\bar{X}^b)$ ), where  $H$  is the  
 14 observation forward operator that transforms values in the model space to those in the  
 15 observation space;  $\tilde{P}^a = \left[ (Y^b)^T R^{-1} Y^b + \frac{(K-1)I}{r} \right]^{-1}$  is the analysis error covariance matrix  
 16 in ensemble space, which is a function of  $Y^b = H X^b$ , the matrix of background ensemble  
 17 perturbations in the observation space,  $R$ , the observation error covariance (e.g.,  
 18 measurement error, aggregation error, representativeness error), and of  $r$ , a multiplicative  
 19 inflation parameter; and  $\tilde{K} = \tilde{P}^a Y^b R^{-1}$ . LETKF assimilates simultaneously all  
 20 observations within a certain distance at each analysis grid point, which defines the  
 21 localization scale. Hunt et al. [2004] introduced a 4-dimensional version, and Hunt et al.  
 22 [2007] provide a detailed documentation of the 4D-LETKF which we are using.

23

## 24 **2.4 Choosing the long observation window (OW) and the short assimilation window** 25 **(AW)**

26 Like other data assimilation methods, LETKF proceeds in analysis cycles that  
 27 consist of two steps, a forecast step and an analysis step. In the analysis step, the model  
 28 forecast (also called prior or background) and the observations are optimally combined to  
 29 produce the analysis (also called the posterior), which is the best estimate of the current  
 30 state of the system under study. In the forecast step, the model is then advanced in time

1 with the analysis as the initial condition and its result becomes the forecast for the next  
2 analysis cycle. All observations within the assimilation time window are used to constrain  
3 the state at the end of the assimilation window.

4 The focus of this study was on the estimation of SCFs that are time varying  
5 parameters in GEOS-Chem. As discussed earlier, a preliminary LETKF analysis, which  
6 provides the weights for each ensemble perturbation, is performed over a longer window  
7 (e.g., 7 days with observations starting at time  $t$ ). Then, the “No-Cost” smoothing [Kalnay  
8 et al, 2007b, Kalnay and Yang, 2010] is applied, using the same analysis weights obtained  
9 at the end of the long observation window (e.g., 7 days) for each ensemble member, but  
10 combining the ensemble perturbations at the end of the corresponding short assimilation  
11 window (e.g., 1-day). This creates the final 1-day analysis (at time  $t+AW$ ), which benefits  
12 from the information from all the observations made throughout the long OW (7 days), and  
13 from the linearity of the perturbations in the short AW of 1 day, which is required for  
14 accuracy. At this time the procedure is repeated starting at  $t+AW$ , one day later.

15 In this new approach, we have the flexibility to combine a short assimilation  
16 window (AW) of length  $m$  (e.g.,  $m=1$  day), with a long observation window (OW) of length  
17  $n$  (e.g.,  $n=7$  days), to improve the estimation of SCF. In the forecast step, the model is  
18 integrated from  $t$  to  $t+n$ , to produce the forecast corresponding to the observations within  
19 the OW. In the analysis step, the observations and corresponding forecasts within the OW  
20 are used by the LETKF to estimate optimal weights for the ensemble members. The “No-  
21 Cost” smoother applies these optimal weights to determine the analysis of the model state  
22 and the SCF parameter at  $t + m$ . The resulting analysis is then used as the initial conditions  
23 for the next analysis cycle starting from time  $t + m$ .

## 25 **2.5 Experimental setup**

26 In our experiments we used an ensemble size of 20 members, which was  
27 reasonable since the data assimilation include only one state variable (CO<sub>2</sub> concentration)  
28 and one parameter variable (SCF). A similar experiment but with 80-member ensemble  
29 size showed only slight improvement of assimilation quality (figure not shown) but  
30 dramatically increased the computational cost. The initial ensemble is created by random  
31 selection of the state and flux values from the model-based “nature” run for both SCF and

1 atmospheric CO<sub>2</sub> concentration. Therefore, the initial uncertainties of fluxes and CO<sub>2</sub>  
2 values are equivalent to their “natural” variability. Based on a sensitivity analysis, we found  
3 a horizontal localization radius of 15000 km is optimal for our system. Following Kang et  
4 al. [2012], a vertical localization is also applied by assigning a larger weight to the CO<sub>2</sub>  
5 updating on surface layers to reflect the expected dominance of layers near the ground in  
6 the change of the total column CO<sub>2</sub> measured by OCO-2.

## 8 **2.6 Additive Inflation Method**

9 The inflation is very important for our LETKF\_C data assimilation system. The  
10 LETKF uses the forecast ensemble spread to represent forecast uncertainties. All EnKFs  
11 tend to underestimate the uncertainty in their state estimate because of nonlinearities and  
12 limited number of ensemble members (Whitaker and Hamill, 2002). Underestimating the  
13 uncertainty (ensemble spread) leads to overconfidence in the background state estimate,  
14 and less confidence in the observations, which will eventually lead the EnKF to ignore the  
15 observations and result in filter divergence. This is also true for our carbon-LETKF data  
16 assimilation system. The ensemble spread of CO<sub>2</sub> in GEOS-Chem model decreases during  
17 model integration when the ensemble members are using the same meteorological forcing  
18 and SCF values, which is very different from the system with prognostic meteorological  
19 fields where the ensemble spread of model state increases during model integration (not  
20 shown). The ensemble spread of SCFs also does not increase during model integration  
21 because the SCFs are predicted using persistence, and the LETKF decreases the ensemble  
22 spreads for both SCFs and CO<sub>2</sub> during analysis steps. Therefore, without inflation, the  
23 ensemble spread of the CO<sub>2</sub> and SCFs would be continuously decreasing during data  
24 assimilation, and soon would become too small for LETKF to accept any observations, and  
25 hence, cause filter divergence.

26 There are different types of inflation methods that address the problem of  
27 overconfidence, such as multiplicative inflation, relaxation to prior, and additive inflation  
28 [e.g. Anderson and Anderson, 1999; Mitchell and Houtekamer, 2000; Zhang et al., 2004;  
29 Whitaker et al., 2008; Miyoshi, 2011]. For this study, we chose additive inflation, which  
30 adds random fields to the analysis before the ensemble forecast of the next analysis cycle.  
31 Additive inflation has some advantages compared to multiplicative inflation because it

1 prevents the effective ensemble dimension from collapsing toward the dominant directions  
2 of error growth [Whitaker et al., 2008; Kalnay et al., 2007a]. We applied additive inflation  
3 to the ensemble of atmospheric CO<sub>2</sub> and SCF to increase perturbations in the initial  
4 conditions, for the next time step. It is important for an additive inflation method to  
5 minimize the impact of model imbalance and initial shocks generated by adding the random  
6 fields into a model. Following Kang et al [2012], the added fields are selected randomly  
7 from the model nature run. Pairs of atmospheric CO<sub>2</sub> and surface CO<sub>2</sub> flux fields are  
8 chosen randomly from model nature run within one year before the analysis time, their  
9 ensemble mean is removed and their difference are scaled to a magnitude corresponding to  
10 30% of model seasonal variance to create the ensemble of random fields for additive  
11 inflation. Therefore, each selected random field is balanced, and when it is added into  
12 model, the balance will be essentially maintained.

13

### 14 **3. Sensitivity analysis for AW and OW length**

15 We tested the new version of the LETKF with short AW and long OW, described  
16 in previous sections by conducting two sets of experiments using the LETKF\_C system in  
17 an OSSE framework with OCO-2 like observations. The first set of experiments used the  
18 regular 4D-LETKF settings (with a single window length AW=OW) to investigate the  
19 effect of the length of AW for estimating SCF. In the second set of experiments, we  
20 investigated the optimal OW length after choosing the best AW from the first set of  
21 experiments. The assimilation period for all experiments was 1 January 2015 to 1 March  
22 2016. The annual mean RMSEs differences are calculated from the simulation results by  
23 removing the spin-up period of first two months (January and February 2015). The average  
24 period is from March 1 2015 to the end of February 2016. The details of experimental  
25 settings are shown in Table 1.

26

27

28

29

30

31

1  
2  
3  
4  
5

Table 1. Lengths of Assimilation Window (AW), and Observation Window (OW), and the resulting time-averaged global mean RMSEs for different experiments. The first four experiments use regular 4D-LETKF, with AW=OW. The last four experiments use AW=1 day, found to be optimal, and different OWs.

	EXP1	EXP2	EXP3	EXP4	EXP5	EXP6	EXP7	EXP8
AW	6 hours	1 day	3 days	7 days	1 day	1 day	1 day	1 day
OW	6 hours	1 day	3 days	7 days	2 days	8 days	15 days	30 days
RMSE ( $\frac{kgC}{m^2yr}$ )	0.077	<b>0.059</b>	0.068	0.074	0.053	<b>0.041</b>	<b>0.040</b>	0.050

6  
7

### 3.1 Sensitivity analysis for different assimilation windows

9           The sensitivity of SCF estimates to the length of AW was investigated based on the first set of experiments (EXP1-EXP4) with regular 4D-LETKF settings, where the length of OW is the same as that of the AW. All experiments used the same observations and initial conditions. Since the temporal coverage of the OCO-2 observation network is too sparse for our LETKF\_C assimilation system to estimate the SCF signal in a short time scales, we focus on the estimation of SCF for the seasonal and longer time scales.

15           Figure 2 shows the estimated global total surface fluxes from the first set of experiments. The “true” global total surface fluxes show a clear seasonal cycle with very large carbon uptake during the growing season of Northern Hemisphere (NH), from May to August, and carbon release during other seasons with the peak release during November. All experiments reproduced fairly well the seasonal cycle of SCF.

20           When the AW is very short (6 hours), there are large magnitude and high frequency noise overlaying the seasonal cycle. The magnitude of high frequency errors of SCF estimation in EXP1 is comparable with the seasonal variability of SCF (Figure 2a). When the AW=7 days, the high frequency errors of estimation decay, but the long assimilation window increases the analysis RMSE (EXP4). The EXP2 with AW= 1 day produced the best estimation of SCF among all four experiments with equal observation and assimilation

1 windows (Figure 2).

2 The advantage of AW=1 day (EXP2) is clearly seen from the smaller average global  
3 root mean square error (RMSE) (Figure 2c). The RMSE of surface carbon flux is calculated  
4 as

$$5 \quad RMSE(t) = \sqrt{E_x((F^a(x, t) - F^n(x, t))^2)} \quad (3)$$

6 where  $x$  and  $t$  are space and time location;  $F^a$  and  $F^n$  indicate the analysis and the “true”  
7 SCF from nature run, respectively.  $E_x$  is spatial average. The estimations from experiments  
8 with long AW (3 days and 7 days) have a smaller RMSE for the first three months (January  
9 to March), when the “truth” had very little variation because the long AWs enhances the  
10 signal and smoothes the high-frequency noise. The experiments with long AW could miss  
11 the fine-scale signals of SCF variation and fail to catch its variation with time. Therefore,  
12 the estimations with long AW showed large RMSE during the period when SCF had larger  
13 variations. The estimation with AW of 6 hour showed very large RMSE because of the  
14 overwhelming high frequency noise. The estimation with AW of 1 day had the smallest  
15 RMSE among all the experiments with regular 4D-LETKF.

16 The time-averaged RMSEs of SCFs is calculated as

$$17 \quad RMSE(x) = \sqrt{E_t((F^a(x, t) - F^n(x, t))^2)} \quad (4)$$

18 which shows very similar spatial patterns, but different amplitudes for different  
19 experiments (Figure 3). The large RMSEs of SCF estimation located in Southeast  
20 American, Southeast of China and Russia, and resembled that of the SCF variance (not  
21 shown). The regions of higher variance indicate more information is needed to resolve such  
22 large variance by observations, which is hard to achieve. As expected, the SCF RMSE of  
23 0.059 from EXP2 with AW of 1 day is significantly smaller than the RMSE from EXP1  
24 with a short AW of 6 hour ( $0.077 \frac{kgC}{m^2yr}$ ), and EXP3 and EXP4 with longer AWs of 3 days  
25 ( $0.068 \frac{kgC}{m^2yr}$ ) and 7 days ( $0.074 \frac{kgC}{m^2yr}$ ) respectively.

26 Our results suggest that the preferred AW for estimating SCF is 1 day. This is  
27 distinctly different from previously published studies that indicate either a very short AW  
28 (6 hours) [Kang et al 2011, 2012], or a very long AW (longer than a few weeks) [e.g.,  
29 Baker et al., 2006, 2010; Peters et al., 2005, 2007; Michalak, 2008; Feng et al., 2009] is

1 optimum. A short AW can better constrain the model state and therefore produce a better  
2 parameter estimation. It is worth mentioning that a very short AW of 6 hours can degrade  
3 the SCF estimation with high frequency noise in our LETKF-C system. We postulate that  
4 the high frequency noise is related to the sampling errors in the CO<sub>2</sub>-SCF covariance that  
5 has smaller signal-noise ratio compared to those in experiments with longer AWs.

6 The same results can be obtained from the same experiments with different initial  
7 time, indicating the robustness of our findings [figure not shown]. The convergence of  
8 estimated SCFs from the experiments starting from months with big SCF variation, such  
9 as April, is slightly slower than the experiments from the time with small SCF variation,  
10 such as January. While the estimated SCFs converges in a few analysis cycles ( a few days)  
11 in our system (Figure 2), the small difference of convergence does not make any significant  
12 impact on the quality of estimated SCFs. Moreover, the calculation of RMSE of estimated  
13 SCFs has excluded the spinup period of first two months to remove the potential impact of  
14 initial condition and initial time.

### 16 **3.2 Sensitivity analysis for different observation windows (OW)**

17 The results presented earlier and associated discussion suggest that parameter  
18 estimation through data assimilation benefits from long training time and having sufficient  
19 number of observations, implying that the length of OW is critical for the estimation of  
20 desired parameter(s). We investigated the effect of such sensitivity to find out the suitable  
21 length of OW for estimating SCF in the second set of experiments (EXP5-EXP8), all based  
22 on the optimum AW=1 day that was identified from the first set of experiments, with  
23 different OW lengths.

24 The estimated global total SCFs in the second set of experiments show a clear  
25 seasonal cycle matching the “truth” (Figure 4a). Compared with EXP2 (OW=1) shown  
26 with the green line in Figure 2a), EXP5 (OW=2days) reduced the high frequency noise  
27 significantly when the OW length was increased from 1 day to 2 days. There is still some  
28 high frequency noise in the SCF estimation for EXP5, because the observations for 2 days  
29 are not sufficient to smooth out the high frequency noise introduced into the estimation  
30 through data assimilation. The estimated global total SCFs for EXP6 (OW=8days), EXP7  
31 (OW=15), EXP8 (OW=30) are much smoother than that of EXP5 (OW=1day), because of

1 their longer OW. However, the estimation for OW of 30 days shows a clear time shift  
2 compared with “truth”, especially during the transient period when the majority of  
3 ecosystems /plants switching from dormant phase in the winter to the growing phase in the  
4 spring. The surface carbon fluxes change rapidly during this period. The time shift can also  
5 be seen in the estimations for these experiments with OW of 15 days, but it is less  
6 pronounced. In the proposed LETKF technique, most of observations in a long OW are  
7 introduced at a time later than the assimilation time. Since the SCFs are temporally  
8 evolving parameters, the information (variation) of future surface fluxes is brought into the  
9 estimation of current time when the future observations are included in the OW. Therefore,  
10 the estimated SCF with a very long OW tend to shift towards its future value. The estimated  
11 SCF with moderate OW=8 days and 15 days (EXP6 and EXP7) are more accurate than  
12 those with a short OW of 2 days (EXP5) and very long OW of 30 days (EXP8), by avoiding  
13 the significant high frequent noise observed in EXP5 (OW=2 days) and the significant time  
14 shift present in EXP8 (OW=30 days). The global mean RMSEs of estimated SCF from  
15 OW=8 and 15 days (EXP6 and EXP7) are significantly smaller than those from OW=2 and  
16 30 days, i.e., EXP5 and EXP8 (Figure 4c).

17 The spatial pattern of time-average RMSE of SCF for EXP5 (OW=2 days; Figure  
18 5) is similar to those in the first set of experiments, which had short AW=OW (Figure 3).  
19 The regions with large RMSE in EXP5 (OW=2 days) disappear with OW=7 and 15 days  
20 in EXP6 and EXP7, because the long OWs enhance the signals for SFC estimation. The  
21 large RMSE in SCF estimates for EXP8 (OW=30 days) are primarily in the Northern  
22 Hemisphere mid-latitudes, because of the time shift in estimations with OW=30 days. The  
23 mean RMSEs of experiments with moderate OWs of 8 and 15 days are  $0.041 \frac{kgC}{m^2yr}$  and  
24  $0.040 \frac{kgC}{m^2yr}$ , respectively, which is significantly smaller than those from experiments with  
25 OWs of 2 days ( $0.053 \frac{kgC}{m^2yr}$ ) and 30 days ( $0.050 \frac{kgC}{m^2yr}$ ).

26 A longer OW requires a longer forecast period for each forecast step, which results  
27 in additional computational time/cost. For example, EXP7 with OW of 8 days used 8-time  
28 more computational time compared to EXP2. Furthermore, the length of OW is also  
29 constrained by the time scale of estimation parameters. A long OW tends to generate a  
30 time shift for its estimation. For seasonal and longer time scales, OW(s) in moderate range



1 of 8~15 days appear to be most suitable for the LETKF\_C estimates of the SCF. EXP6  
2 and EXP7 show almost the same quality of SCF estimation, but EXP6 has higher  
3 computational efficiency. The best configuration thus appears to be EXP6 with an OW of  
4 8 days and AW of 1 day, referred as the “benchmark” experiment hereafter.

5 We note that the high frequency noise in EXP1 with a short AW of 6 hours can be  
6 smoothed out by a long OW (i.e. 8-15 days). We postulate that an experiment with AW of  
7 6 hours and OW 8 days will produce similarly realistic estimations as the “benchmark”  
8 experiment; however, it would require much more computational time.

#### 9 10 **4 Evaluating estimated fluxes from the “benchmark” experiment**

11 With the moderate long observation and short assimilation windows, we obtained  
12 best estimates of surface carbon fluxes, and their seasonal cycle. This section describes the  
13 SCF estimates from the “benchmark” experiment. Figure 6 shows a comparison of surface  
14 carbon fluxes based on the “benchmark” assimilation experiment and nature (“truth”) run  
15 for Northern Hemisphere Summer (June, July and August) and Winter seasons (December,  
16 January, and February). The “bottom-up” carbon fluxes used in the “nature” run show a  
17 very strong seasonal cycle over the continents, except Antarctica. The North Hemisphere  
18 mid-latitude areas are very large carbon sinks in the Summer, and carbon sources in the  
19 Winter, as expected. The strong seasonal cycle of surface fluxes mainly related to the  
20 variability of terrestrial ecosystems that absorbs large amount of CO<sub>2</sub> during the growing  
21 season (Spring and Summer) and release carbon back to the atmosphere during dormant  
22 seasons (Fall and Winter). The estimated surface fluxes in the seasonal time scale follow  
23 closely the “truth”. The benchmark assimilation experiment closely reproduces the spatial  
24 pattern of surface fluxes globally, for different seasons. The difference between the  
25 benchmark estimation and “truth” shown in Figures 6 e & f are very small. There are some  
26 positive carbon flux differences over Northern Hemisphere mid-latitudes in the Winter,  
27 thus a positive bias in estimated atmospheric CO<sub>2</sub> concentration is expected.

28 The analysis of CO<sub>2</sub> concentrations matches the “nature” run well. The error pattern  
29 also matches the CO<sub>2</sub> seasonal cycle and the error pattern of estimated SCF. Figure 7  
30 shows the comparison of surface atmospheric CO<sub>2</sub> concentrations between the benchmark  
31 assimilation experiment and nature (“truth”) run, for the Northern Hemisphere Summer

1 and Winter. The spatial pattern of assimilated CO<sub>2</sub> matches the “truth” very well. The  
2 analysis successfully reproduced the seasonal cycle of CO<sub>2</sub> over Northern Hemisphere  
3 mid-latitudes, with low CO<sub>2</sub> concentration in Summer (Figures 7a-c) and high CO<sub>2</sub> in  
4 Winter (Figures 7b-d), consistent with seasonal cycle of CO<sub>2</sub> absorption and release by  
5 terrestrial ecosystems. There are positive CO<sub>2</sub> concentrations located at high latitudes of  
6 North America and far East Asia regions during Winter 2016 (Figure 7f), due to the positive  
7 bias in estimated SCF (Figure 6f).

8 The consistency of annual mean estimated SCF for both benchmark experiment and  
9 “truth” is a very important feature for our LETKF\_C assimilation system (Figure 8a). In  
10 EnKF assimilation the ensemble spread is considered as a good representation of  
11 uncertainties associated with both parameters and model state [e.g., Evensen 2007, Liu et  
12 al. 2014]. The surface carbon fluxes are special parameters that vary with time and it is  
13 very hard to quantify their uncertainty during assimilation. When the ensemble spread of  
14 parameters are too small to drive model with a robust response, the estimation fails. The  
15 additive inflation with 30% of nature variability is used to maintain the amplitude of  
16 parameters ensemble spread. Although the ensemble spread of the global total surface flux,  
17 in our experiments, is bigger than its error (Figure 8a), we were still able to estimate very  
18 well the global total surface CO<sub>2</sub> fluxes (ensemble mean), and their seasonal variability.  
19 This is consistent with findings of Liu et al [2014], that parameter estimation can tolerate  
20 some inconsistency between parameter ensemble spread and parameter error.

21 The global mean RMSE of SCF decrease from an initial value of  $\sim 0.1$   
22  $kg\ C\ m^{-2}y^{-1}$  to  $\sim 0.04\ kg\ C\ m^{-2}y^{-1}$  in just a few analysis cycles (Figure 8b). It does not  
23 further decrease during following assimilation cycles because the SCF values vary  
24 temporally. The signals added by observations are mainly used to reproduce the temporal  
25 variation of SCF.

26 It is very important for a SCF estimation to reproduce the spatial distribution of the  
27 annual mean of the SCF, since it identifies the carbon sources and sinks in the Earth System.  
28 Though the amplitude of annual mean SCF is much smaller than the seasonal cycle of SCF,  
29 the estimated spatial pattern of annual mean SCF in the benchmark experiment (Eq. 5) is  
30 generally consistent with the “truth” (Figure 9).

$$31 \Delta F(x) = E_t(F^a(x, t)) - E_t(F^n(x, t)) \quad (5)$$

1 In summary, we found that the OSSE experiments using long observation windows  
2 and short assimilation windows resulted in the best estimates of SCF.

### 4 **5 Summary and Discussion**

5 We have developed a LETKF-GEOS-Chem carbon data assimilation (LETKF\_C)  
6 system for estimating the surface carbon fluxes (SCF). The GEOS-Chem atmospheric  
7 transport model is driven by the single realization of meteorology fields from MERRA  
8 reanalysis. The proposed system captured the “true” SCF spatial and temporal variability.  
9 The system performed best with a choice of short assimilation and long observation  
10 windows.

11 The LETKF requires a short assimilation window to avoid an ill-posed condition  
12 caused by the nonlinear processes in the forecast model with a long forecast time. The  
13 parameter estimation favors a long training period and many observations. Based on these  
14 features, we developed a new method to accurately estimate the SCF. The new scheme  
15 separates original assimilation time window into observation (OW) and assimilation (AW)  
16 windows, allowing the flexibility to apply an OW that is different than the AW. Like RIP,  
17 the new technique takes advantage of the “no-cost smoothing” algorithm developed for the  
18 LETKF by Kalnay et al. [2007b] that allows to transport the Kalman Filter solution forward  
19 or backward within the observation window.

20 The new method was applied to the LETKF\_C system in the OSSE mode using a  
21 dataset developed based on the OCO-2 observation characteristics. The sensitivity  
22 experiments for this model-assimilation system demonstrated that the new technique, i.e.  
23 with a short AW and long OW, significantly improves the SCF estimation as compared to  
24 regular 4D-LETKF with identical observation and assimilation windows. The best AW for  
25 SCF estimation is 1 day, which is different from the typical AW of 6 hours used in the  
26 meteorological assimilations. An OW in the range of 8-15 days is required to estimate the  
27 surface carbon fluxes for seasonal and longer time scales. The benchmark experiment with  
28 AW of 1 day and the OW of 8 days successfully reproduced the mean seasonal and annual  
29 SCF.

30 Our working hypothesis was that that the optimal OW for the estimation of SCF  
31 could be reduced with more observations. We examined this hypothesis by using simulated

1 OCO-2 observations and Global View Plus (GV+) observations. Similar to the OCO-2  
2 pseudo-observation, the GV+ pseudo-observations were also generated based on the actual  
3 location, time and corresponding error scale of the GV+ flask observations. The results  
4 show that the AW/OW lengths of 1day /8 day is also optimal with both the OCO-2 and  
5 GV+ observation characteristics. We estimated the SCF using the OCO-2 and GV+  
6 pseudo-observations with the identical experiment settings as the OCO-2 experiments,  
7 except we replace the experiment with very long OW of 30 days with an experiment with  
8 a short OW of 4 days to better evaluate the impact from short OWs. Thus the current  
9 experiments settings are using OW of 2, 4, 8, 15 days.

10 The results from these experiments show that the AW/OW lengths of 1day /8 day  
11 is still optimal for both the OCO-2 and GV+ observation characteristics (Figure 10).  
12 Generally, the time-mean RMSE of estimated SCF with OCO-2 and GV+ (Figure 10) are  
13 smaller than the corresponding estimates for OCO-2 only (Figure 5). The short OW of 2  
14 days performs worse than the moderate OWs of 4 days, 8 days and 15 days. The time-  
15 averaged global mean RMSE is  $0.046 \frac{kgC}{m^2yr}$  for experiments with OW of 2 days (Figure  
16 10a). The time-averaged global mean RMSE is only 0.040, 0.037 and 0.039  $\frac{kgC}{m^2yr}$  for  
17 experiments with OW of 4 days, 8 days and 30 days, respectively (Figure 10 b, c and d).  
18 We only see a slight impact of observation coverage on the optimal OW length. The best  
19 OW appears to be 8~15 days which produce the smallest RMSE when only OCO-2  
20 observations only are assimilated. The smallest RMSE in the experiment is obtained in the  
21 experiment with the best OW of 8 days, when both OCO-2 and GV+ observations are  
22 assimilated into the system.

23 Two different sets experiments (OCO-2 vs OCO-2 and GV+) suggesting the same  
24 optimal OW of 8 days indicates that the observation coverage and observation type is not  
25 the major factor in deciding the length of optimal OW. We speculate that the optimal OW  
26 is mainly decided by the time-scale of model response to the SCF uncertainties because  
27 LETKF constrains parameters (SCF) based on the mapping function of parameter-state  
28 covariance, hence, only the model response to the parameter uncertainties provide the  
29 signal for parameter estimation.

30 It is worth noting that our approach works best for estimating parameters that vary

1 slowly over moderate time scales. It may not be optimum for estimating SCF variation for  
2 short time-scales such as sub-daily to daily because the variations shorter than OWs are  
3 filtered out. Furthermore, we used a coarse spatial resolution ( $4^\circ \times 5^\circ$ ) GEOS-Chem in our  
4 study. We postulate that the optimal AW/OW could be different when a higher spatial  
5 resolution version of GEOS-Chem is used with the proposed assimilation system, because  
6 models with different resolutions response to the SCF may be different. This issue also  
7 merits further exploring in the future.

8 Our new developed short AW and long OW technique is different from the standard  
9 4D-variational method and the 4D-LETKF. The 4D-Var and the 4D-LETKF have been  
10 shown (Bonavita et al. 2015; Hamrud et al 2015) to have an essentially equivalent  
11 performance, and their hybrid blending the complete Kalman Gain matrices of the two  
12 systems in an EnKF framework was comparable to the hybrid ensemble data assimilation  
13 system currently operational at ECMWF, but with lower computational cost. The hybrid  
14 ensemble data assimilation system at ECMWF uses an ensemble of 4D-Var assimilation at  
15 reduced resolution to provide a flow-dependent estimate of background errors for use in  
16 4D-Var assimilation (Bonavita et al. 2015). The short AW and long OW approach can be  
17 used with other Earth system models for parameter estimation, when the parameters have  
18 slow and smooth variations in time and space, and the observations are too limited to  
19 constrain the parameters well.

## 20 21 **6 Code and data availability**

22 This study focused on developing a new methodology for estimating carbon flux  
23 based on a carbon cycle model/data assimilation system. It does not generate any new  
24 dataset. The related code for GEOS-Chem and LETKF can be accessed from  
25 [http://acmg.seas.harvard.edu/geos/doc/man/chapter\\_2.html#DownCode](http://acmg.seas.harvard.edu/geos/doc/man/chapter_2.html#DownCode) and  
26 <https://github.com/takemasa-miyoshi/letkf>, respectively.

## 27 28 **References:**

29 Anderson, J.L.: An ensemble adjustment Kalman filter for data assimilation. *Mon. Wea.*  
30 *Rev.*, 129, 2884–2903, 2001.  
31 Anderson J.L.: A local least squares framework for ensemble filtering. *Mon. Wea. Rev.*,

1 131, 634–642, 2003.

2 Anderson, J. L., and Anderson, S. L.: A Monte Carlo implementation of the nonlinear  
3 filtering problem to produce ensemble assimilations and forecasts, *Mon. Weather Rev.*,  
4 127, 2741–2758, doi:10.1175/15200493(1999)127<2741:AMCIOT>2.0.CO;2, 1999.

5 Asefi-Najafabady, S., Rayner, P. J., Gurney, K. R., McRobert, A., Song, Y., Coltin, K.,  
6 Huang, J., Elvidge, C., and Baugh, K.: A multiyear, global gridded fossil fuel CO<sub>2</sub>  
7 emission data product: Evaluation and analysis of results, *J. Geophys. Res. Atmos.*, 119,  
8 10,213–10,231, doi:10.1002/2013JD021296, 2014.

9 Banks, H.T.: Control and estimation in distributed parameter systems. In: H.T. Banks,  
10 Editor, *Frontiers in Applied Mathematics* vol. 11, SIAM, Philadelphia, pp 227, 1992a.

11 Banks, H.T.: Computational issues in parameter estimation and feedback control problems  
12 for partial differential equation systems. *Physica D* 60, 226-238, 1992b.

13 Baker, D. F., Doney, S. C., and Schimel, D. S.: Variational data assimilation for  
14 atmospheric CO<sub>2</sub>, *Tellus, Ser. B*, 58, 359–365, doi:10.1111/j.1600-0889.2006.00218.x,  
15 2006.

16 Baker, D. F., Bösch, H., Doney, S. C., O’Brien, D., and Schimel D. S.: Carbon source/sink  
17 information provided by column CO<sub>2</sub> measurements from the Orbiting Carbon  
18 Observatory, *Atmos. Chem. Phys.*, 10, 4145–4165, doi:10.5194/acp-10-4145-2010, 2010.

19 Basu, S., Baker, D. F., Chevallier, F., Patra, P. K., Liu, J., and Miller, J. B.: The impact of  
20 transport model differences on CO<sub>2</sub> surface flux estimates from OCO-2 retrievals of  
21 column average CO<sub>2</sub>, *Atmos. Chem. Phys.*, 18, 7189-7215, [https://doi.org/10.5194/acp-](https://doi.org/10.5194/acp-18-7189-2018)  
22 18-7189-2018, 2018.

23 Bey, I., Jacob, D. J., Yantosca, R. M., Logan, J. A., Field, B., Fiore, A. M., Li, Q., Liu,  
24 H., Mickley, L. J., and Schultz M.: Global modeling of tropospheric chemistry with  
25 assimilated meteorology: Model description and evaluation, *J. Geophys. Res.*, 106,  
26 23,073-23,096, 2001.

27 Nassar, R., Napier-Linton, L., Gurney, K.R., Andres, R.J., Oda, T., Vogel, F.R., and Deng,  
28 F.: Improving the temporal and spatial distribution of CO<sub>2</sub> emissions from global fossil  
29 fuel emission data sets, *J. Geophys. Res. Atmos.*, 118, 917-933,  
30 doi:10.1029/2012JD018196, 2013.

31 Bishop, C. H., Etherton, B. J., and Majumdar, S. J.: Adaptive sampling with the ensemble

1 transformation kalman filter. Part i: theoretical aspects. *Mon. Wea. Rev.*, 129, 420–436,  
2 2001.

3 Bosilovich, M. G., Akella, S., Coy, L. et al.: MERRA-2: Initial evaluation of the climate.  
4 Series on Global Modeling and Data Assimilation, NASA/TM, 104606, 2015.

5 Bonavita M. G., Hamrud, M., and Isaksen, L.: EnKF and hybrid gain ensemble data  
6 assimilation. Part II: EnKF and hybrid gain results. *Mon. Wea. Rev.*, 143, 4865–4882,  
7 doi:10.1175/MWR-D-15-0071.1, 2015.

8 Burgers, G., Van Leeuwen, P., Evensen, G.: Analysis scheme in the ensemble Kalman  
9 filter. *Mon. Wea. Rev.*, 126, 1719–1724, 1998.

10 Chevallier, F., Engelen, R. J., Carouge, C., Conway, T. J., Peylin, P., Pickett-Heaps, C.,  
11 Ramonet, M., Rayner, P. J., and Xueref-Remy I.: AIRS-based versus flask-based  
12 estimation of carbon surface fluxes, *J. Geophys. Res.*, 114, D20303,  
13 doi:10.1029/2009JD012311, 2009.

14 Cooperative Global Atmospheric Data Integration Project: Multi-laboratory compilation  
15 of atmospheric carbon dioxide data for the period 1957-2015;  
16 obspack\_co2\_1\_GLOBALVIEWplus\_v2.1\_2016\_09\_02; NOAA Earth System Research  
17 Laboratory, Global Monitoring Division. <http://dx.doi.org/10.15138/G3059Z>, 2016.

18 Crisp, D., Randerson, J. T., Wennberg, P. O., Yung, Y. L., and Kuang, Z.: The Orbiting  
19 Carbon Observatory (OCO) mission, *Adv. Space Res.*, 34, 700–709,  
20 doi:10.1016/j.asr.2003.08.062, 2004.

21 Evensen G.: Sequential data assimilation with a non-linear quasi-geostrophic model using  
22 Monte Carlo methods to forecast error statistics. *J. Geophys. Res.*, 99(C5), 10143–10162,  
23 1994.

24 Enting, I. G.: *Inverse Problems in Atmospheric Constituent Transport*, Cambridge Univ.  
25 Press, New York, doi:10.1017/CBO9780511535741, 2002.

26 Feng, L., Palmer, P. I., Bösch, H., and Dance S.: Estimating surface CO<sub>2</sub> fluxes from space-  
27 borne CO<sub>2</sub> dry air mole fraction observations using an ensemble Kalman filter, *Atmos.*  
28 *Chem. Phys.*, 9, 2619–2633, doi:10.5194/acp-9-2619-2009, 2009.

29 Hamrud M., Bonavita M., and Isaksen, L.: EnKF and Hybrid Gain Ensemble Data  
30 Assimilation. Part I: EnKF Implementation. *Mon Wea Rev*, DOI: 10.1175/MWR-D-14-  
31 00333.1, 2015.

1 Harlim, J. and Hunt, B. R.: Four-dimensional local ensemble transform Kalman filter:  
2 numerical experiments with a global circulation model. *Tellus A*, 59: 731–748.  
3 doi:10.1111/j.1600-0870.2007.00255.x, 2007.

4 Houtekamer, P. L., Mitchell, H. L.: Data assimilation using an ensemble Kalman filter  
5 technique. *Mon. Wea. Rev.*, 126, 796–811., 1998.

6 Hunt, B. R., Kostelich, E., and Szunyogh, I.: Efficient data assimilation for spatiotemporal  
7 chaos: A local ensemble transform Kalman filter, *Physica D*, 230, 112–126,  
8 doi:10.1016/j.physd.2006.11.008, 2007.

9 Liu Y., Liu, Z., Zhang, S., Jacob, R., Lu, F., Rong, X., Wu, S.: Ensemble-Based Parameter  
10 Estimation in a Coupled General Circulation Model. *Journal of climate*, 27, 7151–7162,  
11 2014.

12 Le Quéré, C., Moriarty, R., Andrew, R. M. et al.: Global carbon budget 2014, *Earth Syst.*  
13 *Sci. Data*, 7, 47-85, doi:10.5194/essd-7-47-2015, 2015.

14 Le Quéré C., Andrew, R. M., Canadell, J. G. et al.: Global Carbon Budget 2016, *Earth*  
15 *Syst. Sci. Data*, 8, 605-649, doi:10.5194/essd-8-605-2016, 2016.

16 Lokupitiya, R. S., Zupanski, D., Denning, A. S., Kawa, S. R., Gurney, K. R., and Zupanski  
17 M.: Estimation of global CO<sub>2</sub> fluxes at regional scale using the maximum likelihood  
18 ensemble filter, *J. Geophys. Res.*, 113, D20110, doi:10.1029/2007JD009679, 2008.

19 Kalnay E., Li, H., Miyoshi, T., Yang, S.-C., and Ballabrera-Poy, J.: 4-D-Var or ensemble  
20 Kalman filter?. *Tellus, Ser. A*, 59, 758–773, doi:10.1111/j.1600-0870.2007.00261.x, 2007a.

21 Kalnay E., Li, H., Miyoshi, T., Yang, S.-C., and Ballabrera-Poy, J.: Response to the  
22 discussion on “4-D-Var or EnKF?” by Nils Gustafsson. *Tellus, Ser. A*, 59, 778-780, doi:  
23 10.1111/j.1600-0870.2007.00263.x, 2007b.

24 Kalnay, E. and Yang, S.-C.: Accelerating the spin-up of Ensemble Kalman Filtering. *Q.J.R.*  
25 *Meteorol. Soc.*, 136: 1644–1651. doi:10.1002/qj.652, 2010.

26 Kang, J.-S., Kalnay, E., Liu, J., Fung, I., Miyoshi, T., and Ide, K.: “Variable localization”  
27 in an ensemble Kalman filter: Application to the carbon cycle data assimilation, *J. Geophys.*  
28 *Res.*, 116, D09110, doi:10.1029/2010JD014673., 2011.

29 Kang J.-S., Kalnay, E., Miyoshi, T., Liu, J., Fung, I.: Estimation of surface carbon fluxes  
30 with an advanced data assimilation methodology: SURFACE CO<sub>2</sub> FLUX ESTIMATION.  
31 *Journal of geophysical research*, 117., doi:10.1029/2012JD018259, 2012.



1 Mitchell, H. L., and Houtekamer, P. L.: An adaptive ensemble Kalman filter. *Mon. Wea.*  
2 *Rev.*, 128, 416–433, 2000.

3 Michalak, A. M.: Adapting a fixed-lag Kalman smoother to a geostatistical atmospheric  
4 inversion framework, *Atmos. Chem. Phys.*, 8, 6789–6799, 2008.

5 Miyoshi, T.: The Gaussian approach to adaptive covariance inflation and its  
6 implementation with the local ensemble transform Kalman filter. *Mon. Wea.*  
7 *Rev.*, 139, 1519–1535, doi:10.1175/2010MWR3570.1, 2011.

8 O'Dell, C. W., Connor, B., Bösch, H., O'Brien, D., Frankenberg, C., Castano, R., Christi,  
9 M., Eldering, D., Fisher, B., Gunson, M., McDuffie, J., Miller, C. E., Natraj, V., Oyafuso,  
10 F., Polonsky, I., Smyth, M., Taylor, T., Toon, G. C., Wennberg, P. O., and Wunch, D.: The  
11 ACOS CO<sub>2</sub> retrieval algorithm – Part 1: Description and validation against synthetic  
12 observations, *Atmos. Meas. Tech.*, 5, 99–121, doi:10.5194/amt-5-99-2012, 2012

13 Peters, W., Miller, J. B., Whitaker, J., Denning, A. S., Hirsch, A., Krol, M. C., Zupanski,  
14 D., Bruhwiler, L., and Tans, P. P.: An ensemble data assimilation system to estimate CO<sub>2</sub>  
15 surface fluxes from atmospheric trace gas observations, *J. Geophys. Res.*, 110, D24304,  
16 doi:10.1029/2005JD006157, 2005.

17 Peters, W., Jacobson, A.R., Sweeney, C. et al.: An atmospheric perspective on North  
18 American carbon dioxide exchange: Carbon tracker, *Proc. Natl. Acad. Sci. U. S. A.*, 104,  
19 18,925–18,930, doi:10.1073/pnas.0708986104, 2007.

20 Tippett, M., Anderson, J. L., Bishop, C. H., Hamill, T. M., Whitaker, J. S.: Ensemble square  
21 root filters. *Mon. Wea. Rev.*, 131, 1485–1490, 2003.

22 Wang, S., Xue, M., Schenkman, A. D., and Min, J.: An iterative ensemble square root  
23 filter and tests with simulated radar data for storm scale data assimilation. *Quart. J. Roy.*  
24 *Meteor. Soc.*, 139, 1888-1903, 2013.

25 Whitaker, J. S., and Hamill, T. M.: Ensemble data assimilation without perturbed  
26 observations. *Mon. Wea. Rev.*, 130, 1913–1924., 2002.

27 Whitaker J. S., Wei, X., Song, Y., and Toth, Z.: Ensemble data assimilation with the NCEP  
28 global forecast system. *Mon. Wea. Rev.*, 136, 463–482, 2008.

29 Yang, S., Kalnay, E., and Miyoshi T.: Accelerating the EnKF Spinup for Typhoon  
30 Assimilation and Prediction. *Wea. Forecasting*, 27, 878–897,  
31 <https://doi.org/10.1175/WAF-D-11-00153.1>, 2012.

32 Yokota, T., Oguma, H., Morino, I., and Inoue, G.: A nadir looking SWIR FTS to monitor

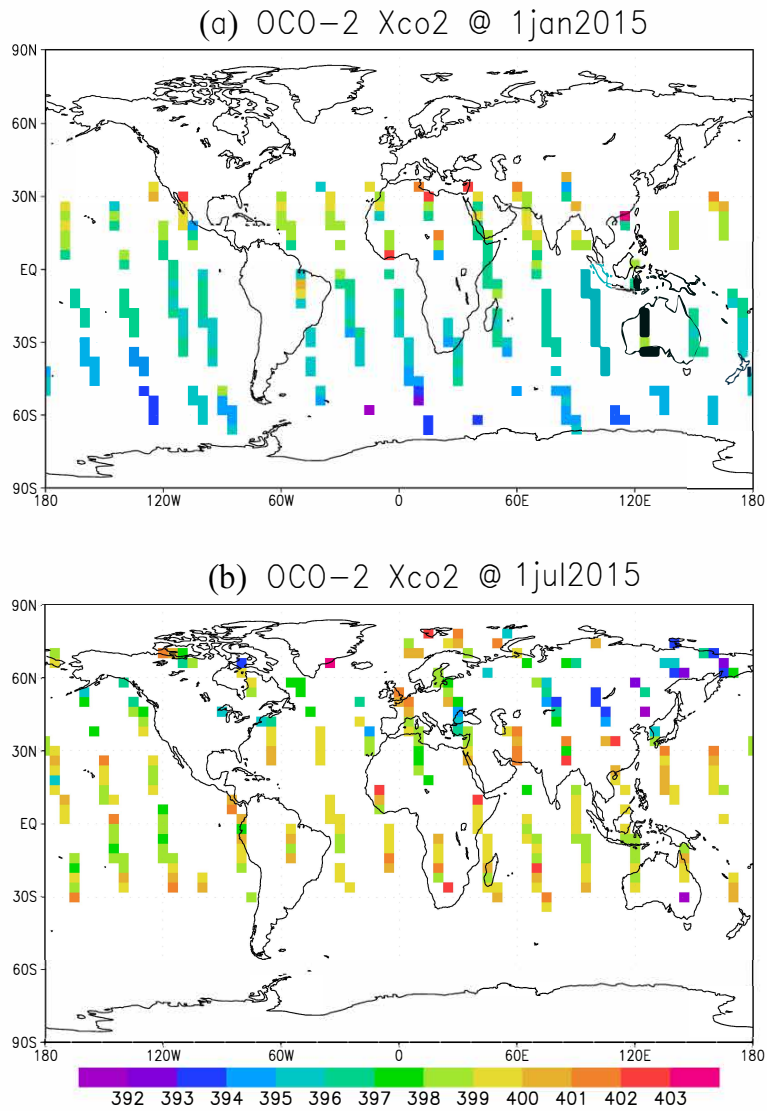
1 CO<sub>2</sub> column density for Japanese GOSAT project, in Proceedings of the Twenty-fourth  
2 International Symposium on Space Technology and Science (Selected Papers), pp. 887–  
3 889, Jpn. Soc. for Aeronaut. and Space Sci., Tokyo, 2004.

4 Zeng, N., Mariotti, A., and Wetzel, P.: Terrestrial mechanisms of interannual CO<sub>2</sub>  
5 variability, *Global Biogeochemical Cycles*, 19, GB1016, doi:10.1029/2004GB002273,  
6 2005

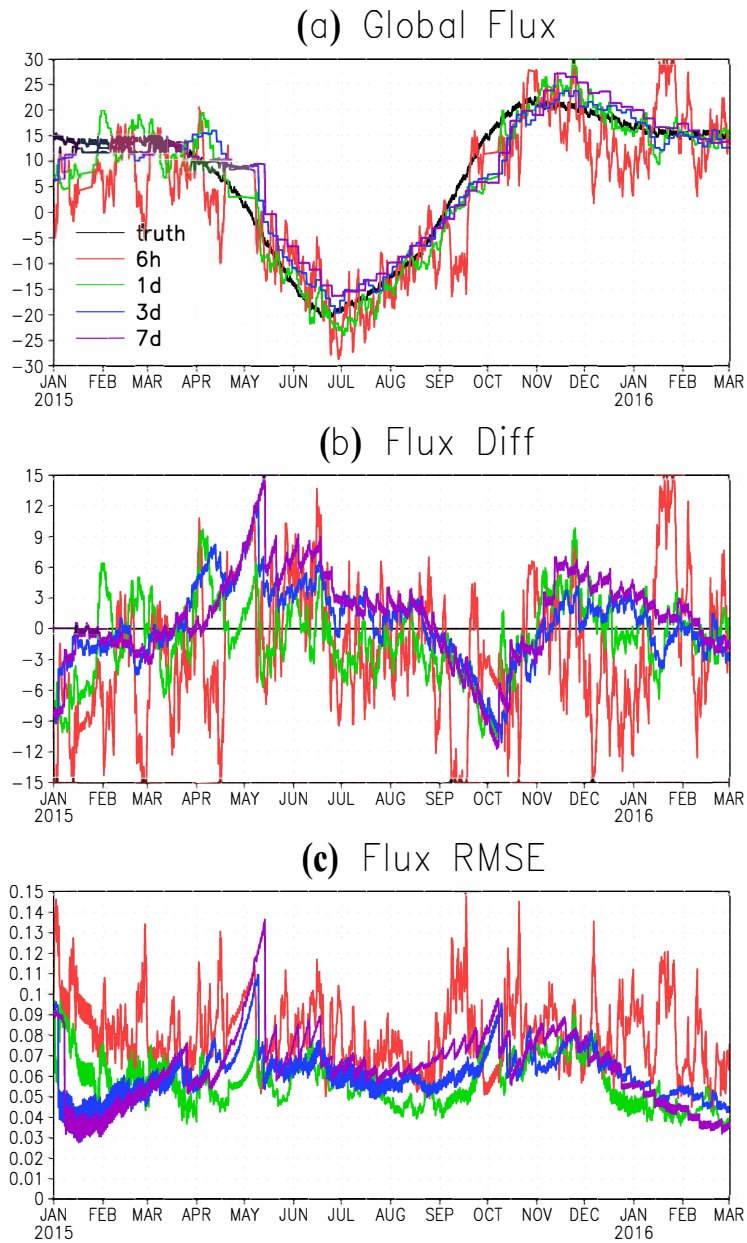
7 Zeng, N., Qian, H., Munoz, E., and Iacono, R.: How strong is carbon cycle-climate  
8 feedback under global warming? *Geophys. Res. Lett.*, 31 L20203,  
9 doi:10.1029/2004GL020904, 2004.

10 Zhang, F., Snyder, C., and Sun, J.: Impacts of initial estimate and observation availability  
11 on convective-scale data assimilation with an ensemble Kalman filter. *Mon. Wea. Rev.*,  
12 132, 1238–1253, 2004.

13 Zupanski, D., Denning, A. S., Uliasz, M., Zupanski, M., Schuh, A. E., Rayner, P. J., Peters,  
14 W., and Corbin, K. D.: Carbon flux bias estimation employing Maximum Likelihood  
15 Ensemble Filter (MLEF), *J. Geophys. Res.*, 112, D17107, doi:10.1029/2006JD008371.  
16 2007.

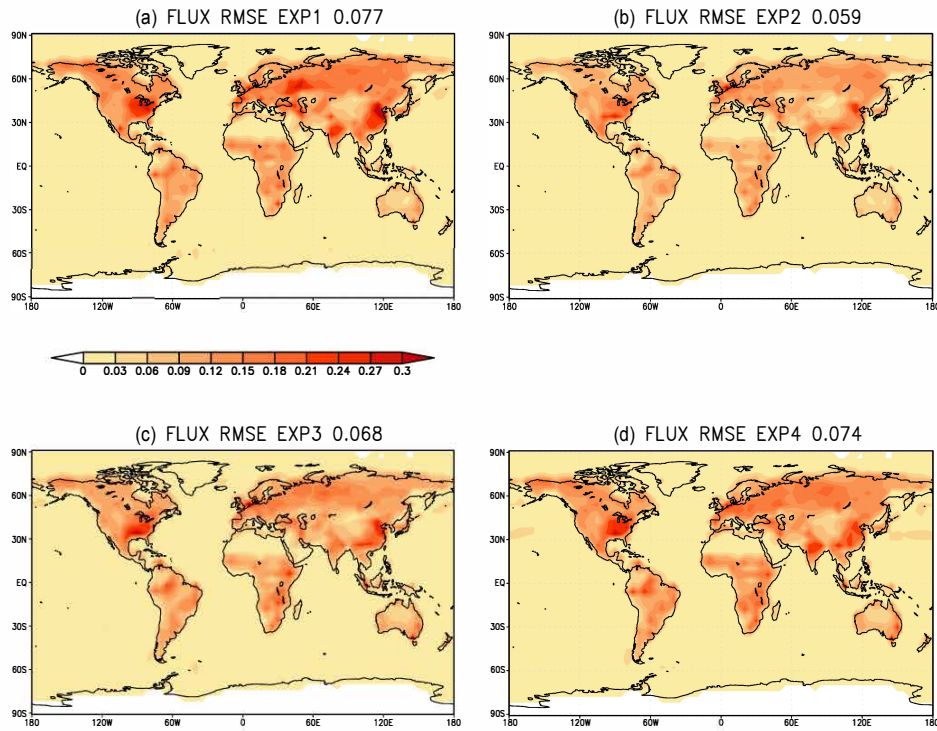


1  
 2 Figure 1. The 10-seconds average of good quality OCO-2 Xco2 observations (Warning  
 3 Level  $\leq 15$ ), obtained from David Baker for (a) 1 January 2015 and (b) 1 July 2015.  
 4  
 5



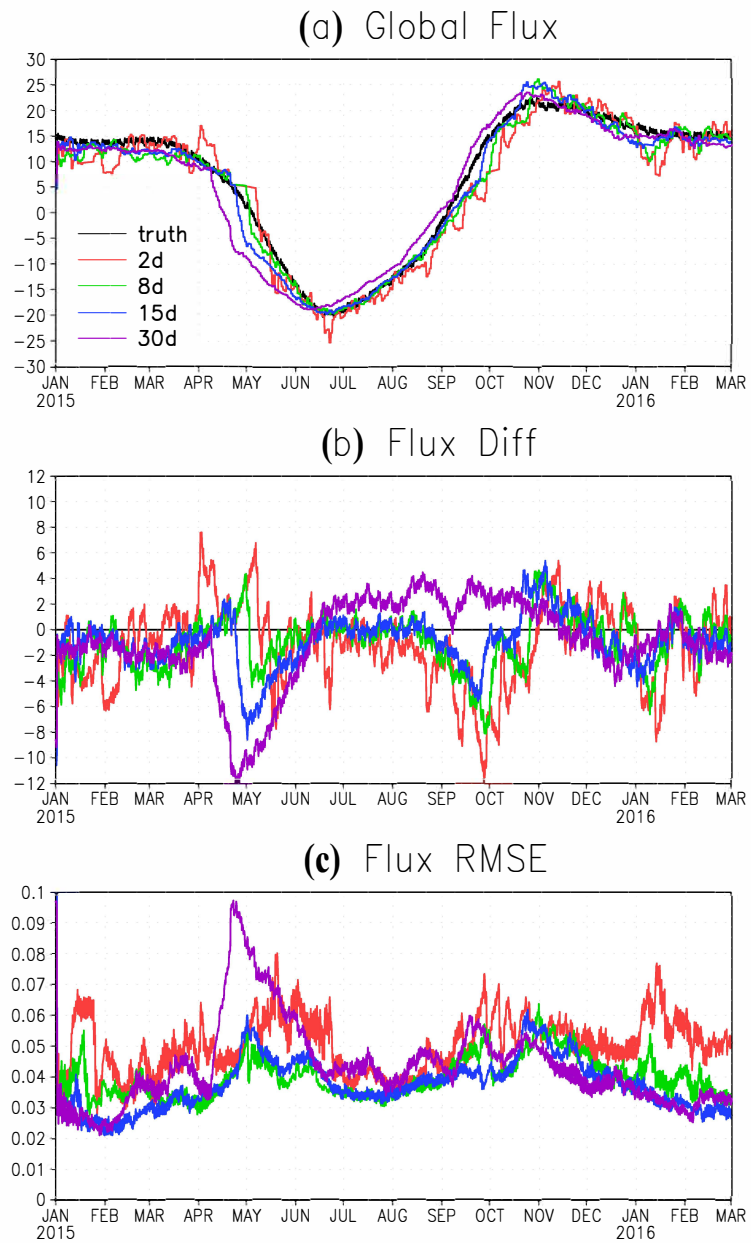
1  
 2 Figure 2. (a) the global total SCF from nature run (“truth”, black line) and from the  
 3 estimations of the first set of experiments with different AW. (b) the difference of global  
 4 total SCF between the estimations from the experiments with different AW and the nature  
 5 run (“truth”). (c) the global average RMSE of the estimated SCFs from the experiments  
 6 with different AW.  
 7

Fnet RMSE of AW 6h/1d/3d/7d 06z01mar2015–01mar2016



1  
2 Figure 3. The spatial pattern of the annual mean RMSE of estimated SCF from the  
3 experiments with different AW (EXP1-4) for the average period from 1 March 2015 to  
4 the end of February 2016. (January and February 2015 are treated as spinup period for our  
5 experiments).  
6

1



2

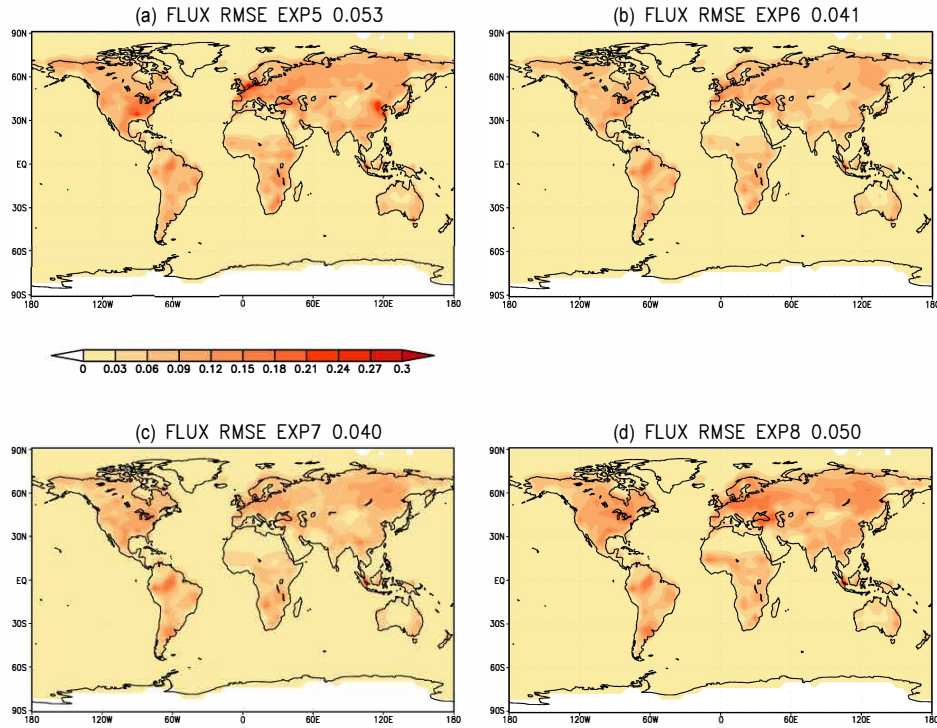
3 Figure 4. Same as Figure 2, except for the second set of experiments with different OW,

4 but same AW of 1 day.

5

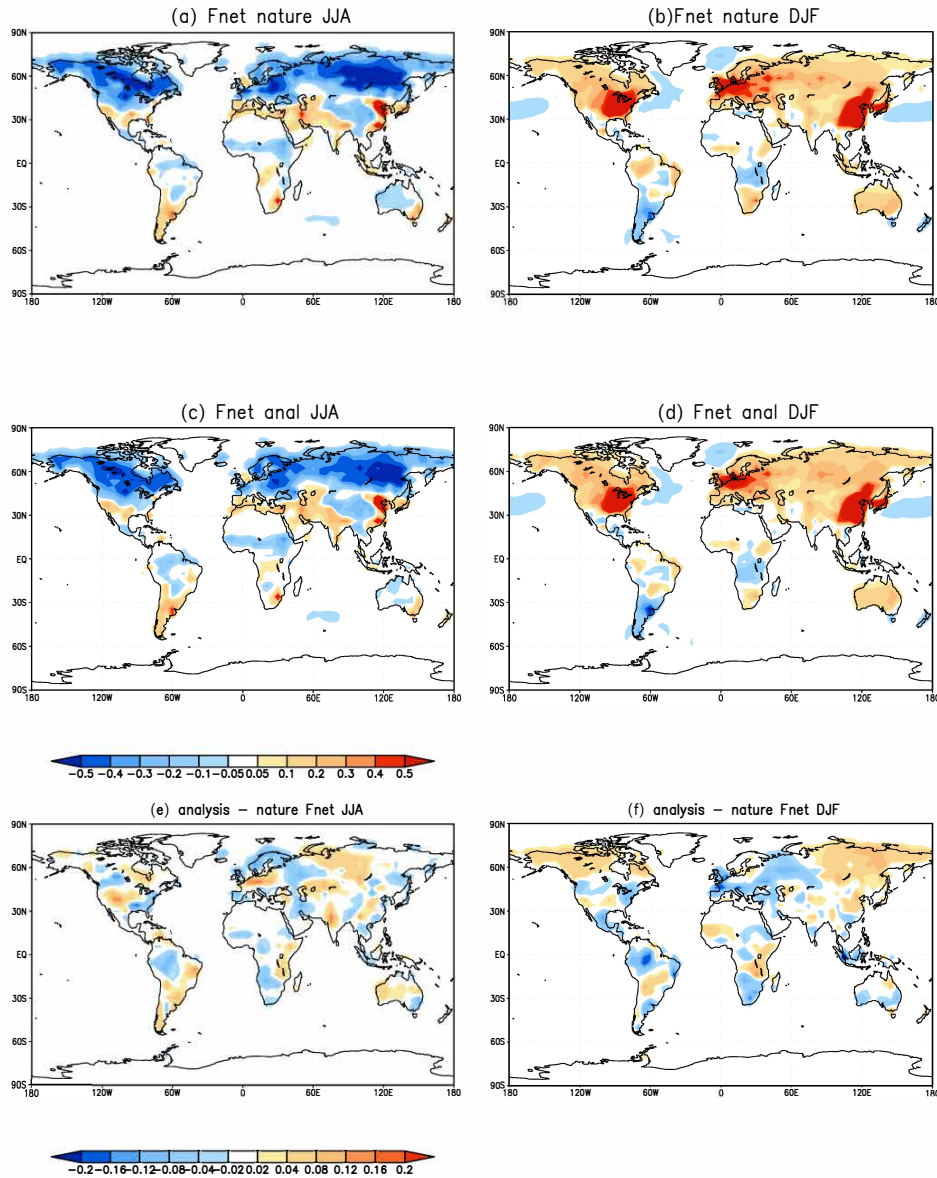
1

**Fnet RMSE of OW 2d/8d/15d/30d 06z01mar2015–01mar2016**



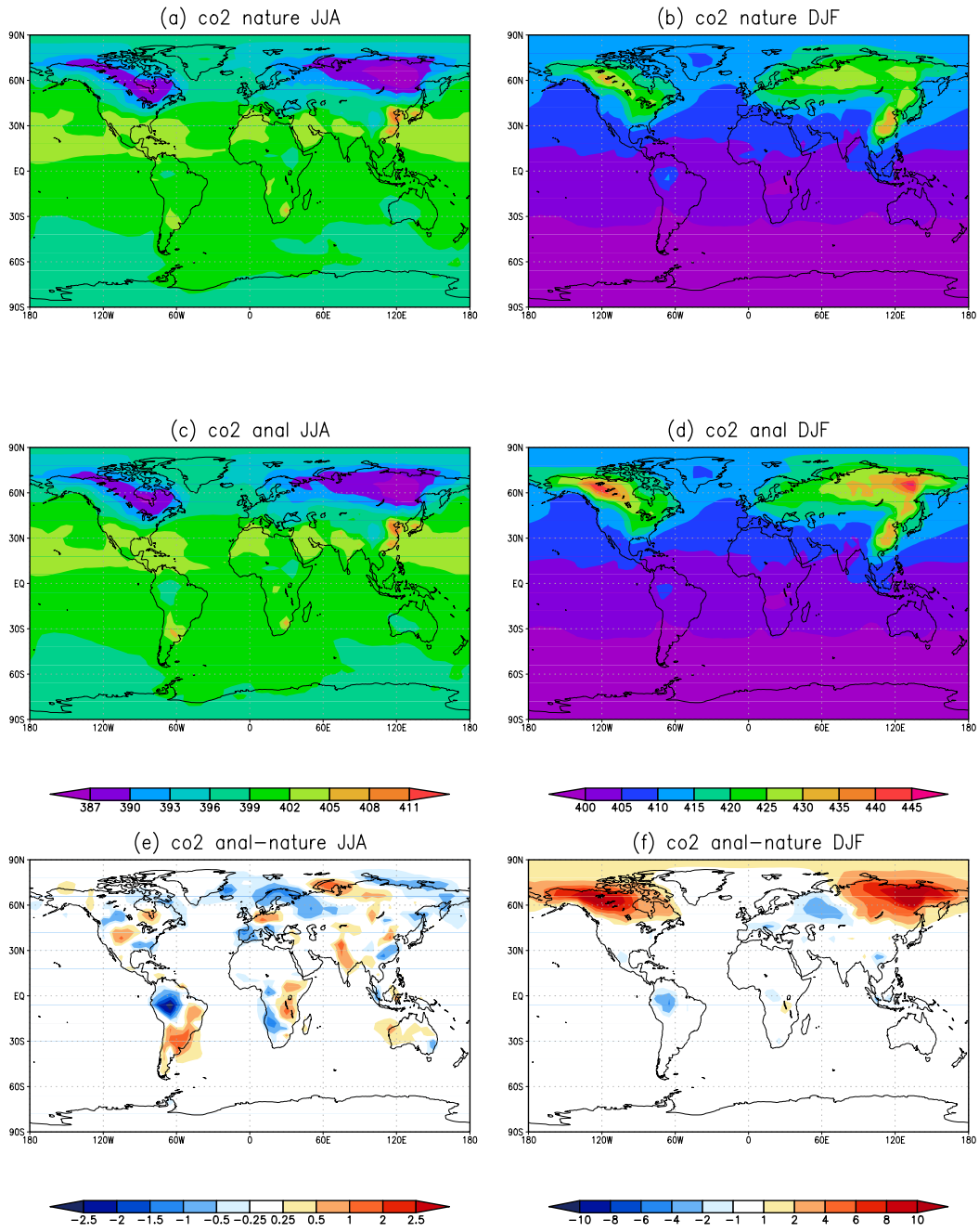
2  
3  
4  
5  
6  
7

Figure 5. Same as Figure 3, except for the second set of experiments with different OW, but similar AW of 1 day.

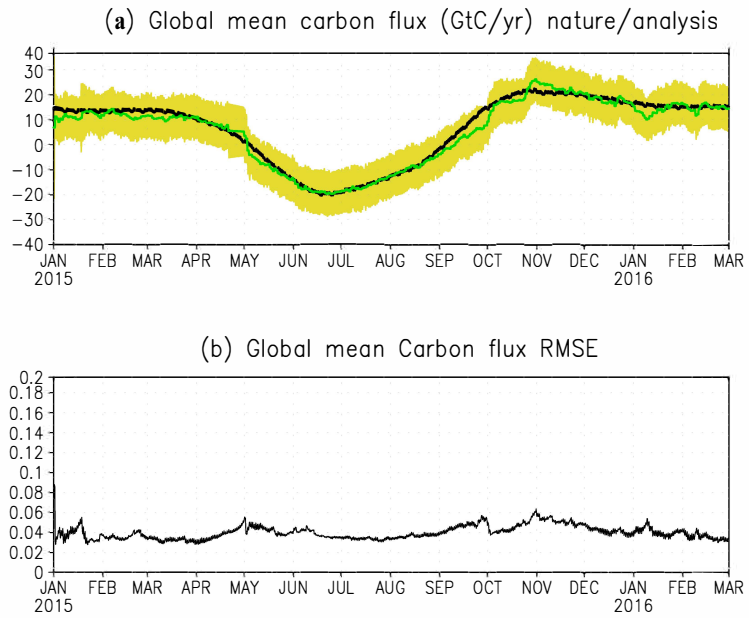


1  
 2 Figure 6. The SCF of "nature" run and estimation from benchmark experiment for Northern  
 3 Hemisphere Summer (a, c and e), and Winter (b, d, and f). The a and b are the "truth" from  
 4 the "nature" run; the c and d are the estimates from benchmark experiment; and the e and  
 5 f are the difference between estimation and "truth".  
 6

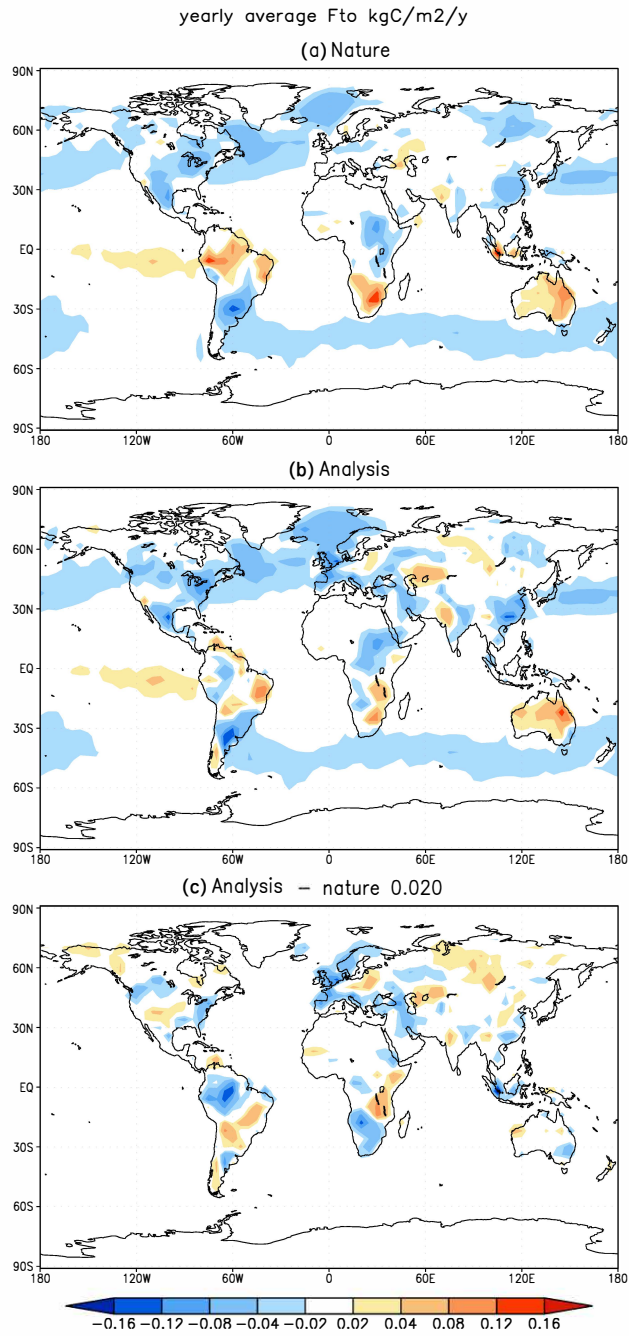




1  
 2 Figure 7. Same as Figure 6, except for surface concentrations of CO<sub>2</sub>. Where (a) and (c)  
 3 share the upper left colorbar; (b) and (d) use the upper right colorbar.  
 4



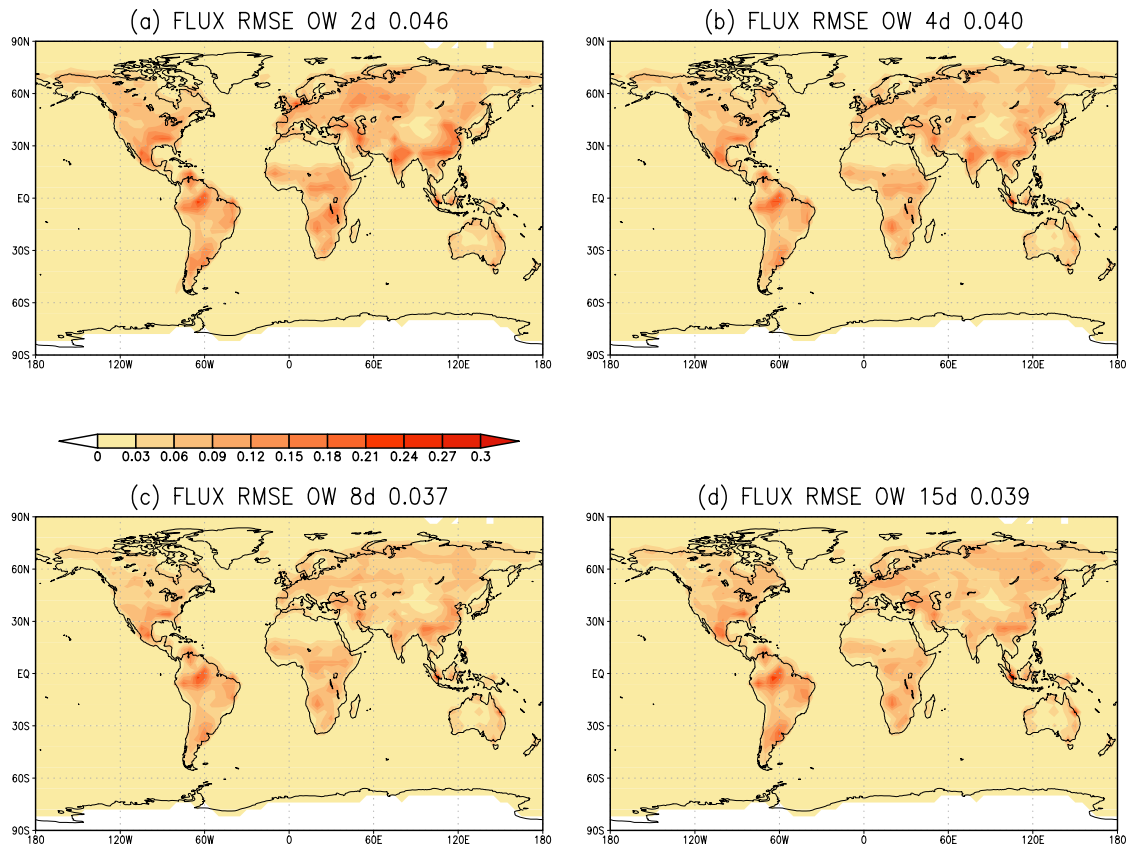
1  
 2 Figure 8. (a) The global total SCF of “truth” and estimation from the benchmark  
 3 experiment: the black line is the truth, green line is the ensemble mean of the estimation,  
 4 and yellow shading is the ensemble spread. (b) the global mean RMSE of the estimated  
 5 SCF from the benchmark experiment.  
 6



1  
 2 Figure 9. (a) the annual mean of SCF (with the FFE removed) for “nature” run; (b) the  
 3 annual mean of estimated SCF (with the FFE removed) from benchmark experiment ; and  
 4 (c) their differences.  
 5  
 6  
 7

1  
2  
3

Fnet RMSE of OW 2d/4d/8d/15d using OCO2 and GV+



4  
5 Figure 10. Same as Figure 5, except for assimilating both OCO-2 and GV+ Pseudo-  
6 Observations. The panel (a), (b), (c) and (d) show the results with OW of 2 days, 4 days,  
7 8 days and 15 days respective.